Frontiers of Materials Science

Electronic Supplementary Material

Fabrication and characterization of photochromic microencapsulated phase change materials with highly cross-linked polyurethane shell coated by nano-TiO_2

Hang Zhang, Shuhui Liu, Xingxiang Zhang, and Wei Li (✉)

School of Material Science and Engineering, Tiangong University, Tianjin 300387, China

E-mail: liwei@tiangong.edu.cn

Materials

Table S1 presents a categorized list of materials employed in this study, along with their functions and purposes, to enhance reader clarity.

Table S1 Materials used in the research and their functions and purposes

Material	Purpose
Ethyl stearate (ES)	Phase change energy storage core material for microcapsules (solvent for photo-variable dyes)
Isophorone diisocyanate (IPDI)	Monomer for cross-linked polyurethane shells
Hexamethylene diisocyanate trimer (HDIt)	Monomer for cross-linked polyurethane shells
Xylitol	Monomer for cross-linked polyurethane shells
Nano-sized titanium dioxide sol (nano-TiO_2 sol)	Emulsifier for Pickering emulsions
Spiropyran (SP)	Photochromic dye
Organic bismuth catalyst	Accelerates the synthesis of cross-linked polyurethanes (reduces side reactions)
Citric acid	Adjust the pH of the emulsion
Sodium hydroxide	Adjust the pH of the emulsion

Characterization

Pickering emulsion droplets were observed at room temperature using a light microscope (OM, MSD701, Phoenix, China) and recorded with the built-in camera.

The surface micromorphology of the microcapsules was observed with field emission scanning electron microscopy (FE-SEM, Gemini 500, Carl Zeiss, Germany) at an accelerating voltage of 10.0 kV. A drop of the diluted microencapsulated emulsion was placed on the sample stage, dried under vacuum at 50 °C, then placed in a vacuum, and a layer of gold was deposited under argon flushing using EMITECH K450× sputtering coating (UK).

The characteristics of microencapsulated phase change materials (MPCMs) were evaluated by differential scanning calorimetry (DSC, Netzsch 200F3). After removing the effects of the previous thermal history, each sample was scanned from room temperature to 80 °C at a rate of 10 °C·min^{-1} in a nitrogen atmosphere.

The chemical structure of the microcapsules, as well as their core and shell, was characterized by Fourier transform infrared spectroscopy with a Nicolet IS-10 spectrometer (Shanghai, China) within a wavenumber range of 4000–500 cm^{-1}. A total of 32 scans were conducted with a resolution of 4 cm^{-1}.

The thermal stability of the microcapsules and their shells was determined by a thermogravimetric analyzer (TGA, STA449F3, Netzsch, Germany). In the TG test, the thermal stability from room temperature to 800 °C was tested in a nitrogen atmosphere with a heating rate of 10 °C·min^{-1} after eliminating the thermal history.

UV–Vis absorption spectra of the microcapsules were obtained using a UV–Vis spectrophotometer (Lambda 35, PerkinElmer Co. Ltd.). The UV–Vis absorption spectra of the microcapsules were obtained. The scanning range was 400–700 nm. The isomerization reaction of SP was excited with a UV lamp (10 W·m^{-2}, 365 nm, Semi Co. Ltd.). The visible light source is an ordinary white LED lamp (10 W·m^{-2}). The test was performed at room temperature.

The ultraviolet–visible–near infrared spectrometer measures was used to measure the UV absorption spectrum of a microencapsulated powder. The scanning range is 230–600 nm.

Impact of nano-TiO_2 concentration on microcapsule thermal stability

To investigate the effect of the nano-TiO_2 concentration on thermal properties of microcapsules, phase transformation characteristics were analyzed by DSC, and the results are revealed in Fig. S1, with thermal performance data summarized in Table S2. It is shown that the fusion and crystallization enthalpies of pure ES are 156.9 and 155.6 J·g^{-1}, respectively. The melting and crystallization curves display a bimodal distribution, attributed to the α-phase of ES molecules and the formation of β crystallites. With the increase in the concentration of the nano-TiO_2 sol, the melting and crystallization enthalpies of microcapsules initially rise, then decrease. The initial increase in enthalpy is attributed to the reduction in the microcapsule particle size with increasing the nano-TiO_2 concentration, which limits the crystallization. The subsequent decrease in enthalpy results from the reaction between the hydroxyl group on nano-TiO_2 and the isocyanate group, which disrupts the polyurethane crosslinking, weakening the shell material and causing the core material leakage. At a nano-TiO_2 sol dosage of 5 g, the maximum melting and crystallization enthalpy values for TPT-MPCMs are 105.1 and 106.2 J·g^{-1}, respectively.

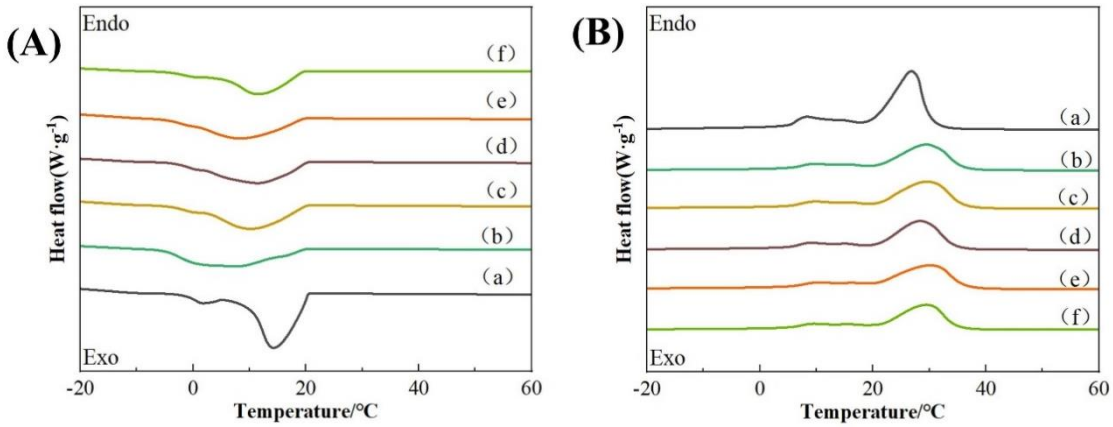

Fig. S1 DSC curves of ES with different added dosages of the nano-TiO_2 sol at 0 g (a), 1 g (b), 5 g (c), 10 g (d), 15 g (e), and 20 g (f) for TPT-MPCMs: **(A)** crystallization curves; **(B)** melting curves.

Table S2 Thermal performances of ES with different added dosages of the nano-TiO_2 sol at 0 g (a), 1 g (b), 5 g (c), 10 g (d), 15 g (e), and 20 g (f) for TPT-MPCMs

Sample	Melting/°C				ΔH_m/(J·g^{-1})	Crystallization/°C		ΔH_c/(J·g^{-1})
	$T_{m,0}$	$T_{m,\alpha}$	$T_{m,\beta}$	$T_{m,\gamma}$		$T_{c,0}$/°C	T_c/°C	
(a)	−1.5	8.4		27.1	156.9	−9.2	14.3	155.6
(b)	−2.1	9.6	15.4	29.3	99.7	−11.5	6.4	98.05
(c)	−3.1	9.7	15.6	29.5	105.1	−12.2	10.0	106.2
(d)	−2.3	9.0	15.0	28.2	101.1	−12.5	11.2	101.7
(e)	−2.9	10.2	16.1	30.0	99.5	−13.4	8.3	99.7
(f)	−2.1	9.4	15.5	29.4	89.5	−11.3	11.4	88.1

Effect of IPDI-to-HDIt ratio on SP UV absorption

To further investigate the effect of the shell material on SP UV absorption, microcapsules with a uniform nano-TiO_2 content of 10 g were prepared, and their visible light absorption spectra were analyzed under 365 nm UV irradiation for 0–100 s. The results are shown in Fig. S2. It is evident that the content of HDIt in the shell material influences the absorbance of the microcapsules. By comparison in Fig. S2(f), it can be observed that the absorption peak of the microcapsules remains stable at 530 nm, despite variations in the IPDI:HDIt ratios, as long as the nano-TiO_2 sol concentration is maintained. This suggests that the absorption of the UV light by microcapsules is more consistent and specific when the nano-TiO_2 concentration is unchanged. Compared to microcapsules with an IPDI:HDIt ratio of 10:0, the addition of HDIt does not significantly affect the absorbance. However, the microcapsule prepared with the IPDI:HDIt ratio of 8:2 exhibits a significantly higher absorbance than those prepared with other ratios. This may be due to that the cross-linked polyurethane formed by the reaction between the shell material and xylitol at an IPDI:HDIt ratio of 8:2 is more transparent, resulting in the minimal impact on the light transmittance of the capsule.

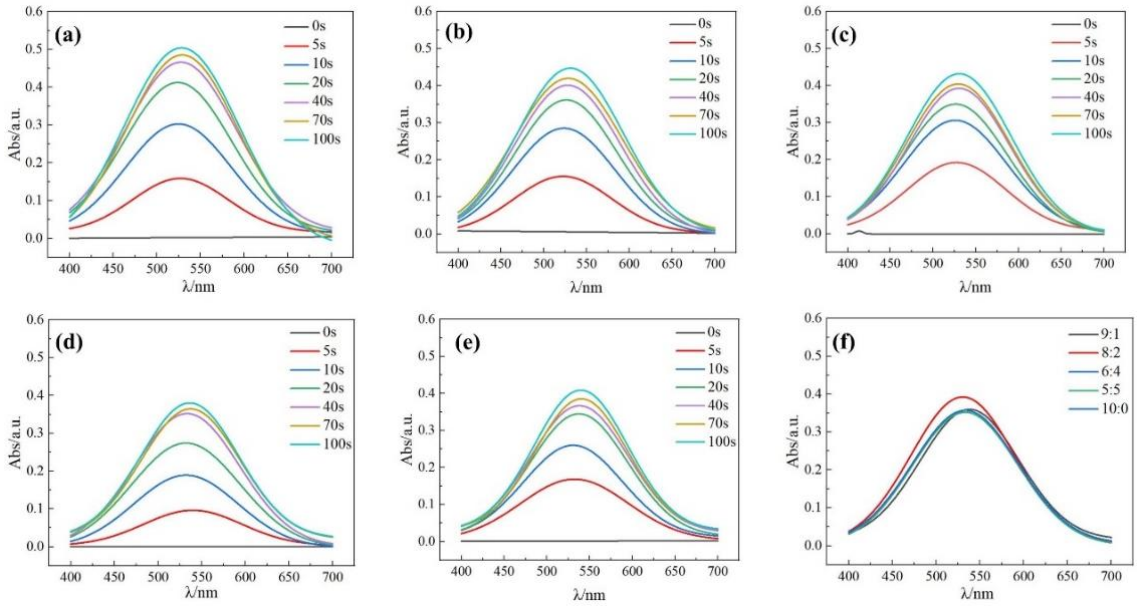

Fig. S2 Visible absorbances of TPT-MPCMs prepared at different IPDI-to-HDIt ratios of **(a)** 9:1, **(b)** 8:2, **(c)** 6:4, **(d)** 5:5, and **(e)** 10:0 under 365 nm ultraviolet light for different durations. **(f)** Absorbances of TPT-MPCMs prepared at different IPDI-to-HDIt ratios under 40 s ultraviolet irradiation.

Effect of IPDI-to-HDIt ratio on DSC behaviors

With the increase in the content of HDIt (i.e., the decrease of the IPDI:HDIt ratio), the enthalpy of the phase change for TPT-MPCMs decreases gradually, as summarized in Table S3. When the IPDI:HDIt ratio is 9:1, the microcapsule shows the best heat storage performance, and the melting enthalpy and crystallization enthalpy are 102.2 and 103.5 $J \cdot g^{-1}$, respectively. When the ratio is 8:2, the enthalpies of fusion and crystallization decrease slightly, which are 100.2 and 102.2 $J \cdot g^{-1}$, respectively. When the ratios are 6:4 and 5:5, the enthalpies of the phase change are further reduced.

Table S3 DSC data of TP-MPCMs prepared with IPDI-to-HDIt ratios of 9:1 (a), 8:2 (b), 6:4 (c), and 5:5 (d)

Sample	Melting/°C				$\Delta H_m/(J \cdot g^{-1})$	Crystallization/°C			$\Delta H_c/(J \cdot g^{-1})$
	$T_{m,0}$	$T_{m,\alpha}$	$T_{m,\beta}$	$T_{m,\gamma}$		$T_{c,0}$	$T_{c,\alpha}$	$T_{c,\beta}$	
(a)	−1.9	8.7	14.8	27.7	102.2	−9.9		6.1	103.5
(b)	−2.2	8.3	14.7	27.6	100.2	−10.4	2.6	10.1	102.2
(c)	−0.9	8.9	15.2	27.8	97.3	−13.6	2.1	8.2	98.8
(d)	−2.1	8.1	15.0	26.3	96.2	−9.4		9.9	97.9

It is worth noting that the DSC curve analysis can reveal the significant effect of the HDI content on crystallization behaviors of microcapsules. As can be seen in Fig. S3(A), when the IPDI:HDIt ratio is 9:1, the crystallization property of the microcapsule is similar to that of pure phase change materials, as shown by Curve (a), showing a single crystal peak. However, at the IPDI:HDIt ratio of 8:2, the crystallization peak of the microcapsule begins to change from single peak to double peaks, which indicates that the crystallization behavior has changed. This may be due to the addition of HDIt, which makes the core material system too viscous, so that some HDIt cannot participate in the cross-linking reaction, staying in the core material. Residual HDIt may act as a heterogeneous nucleation point, interfering with the crystallization process of ES.

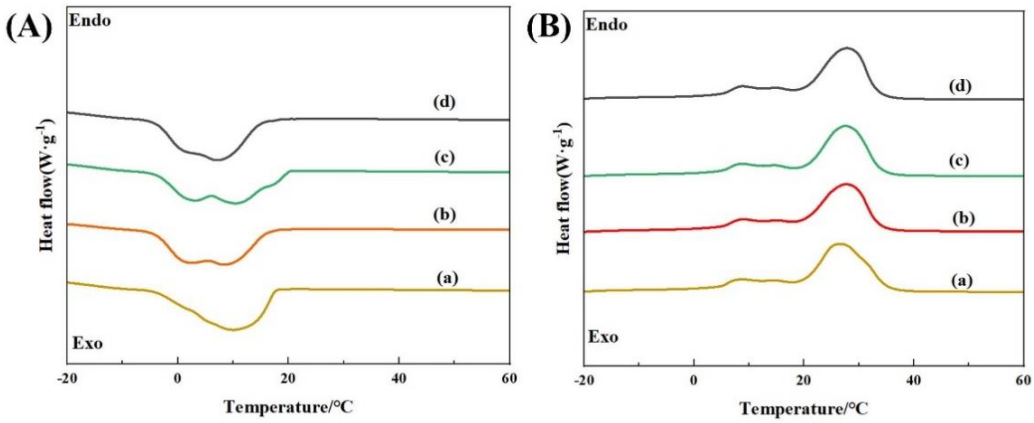

Fig. S3 DSC results of TP-MPCMs prepared with IPDI-to-HDIt ratios of 9:1 (a), 8:2 (b), 6:4 (c), and 5:5 (d): **(A)** crystallization curves; **(B)** melting curves.

Direction for usage of materials

In the field of intelligent packaging, this material can play an important role for products that are sensitive to the UV light and require controlled storage temperatures, such as fresh food and

pharmaceuticals. Its excellent UV absorption performance (with a light absorption rate of 1.0 in the UV band below 350 nm) can effectively block the UV damage to products inside the packaging, preventing the product deterioration caused by the UV irradiation. Meanwhile, its good phase change energy storage capacity (melting enthalpy of 116.2 $J \cdot g^{-1}$ and crystallization enthalpy of 117 $J \cdot g^{-1}$) can maintain the relative stability of the internal temperature of the packaging, reducing the impact of external temperature fluctuations on products. Moreover, the photochromic property of the material under the UV irradiation can serve as an intuitive indicator signal, indicating whether the packaging has been exposed to the strong UV irradiation and helping to judge the quality of the product storage environment.

In the field of energy-saving buildings, this material can be applied to door and window glass coatings or wall paints of buildings. When exposed to the UV light, its photochromic property can adjust the intensity of light entering the room, reducing the input of light and heat into the room in summer. Its phase change energy storage capacity can absorb or release heat when the temperature changes, which helps maintain stable indoor temperatures and reduce the energy consumption of temperature control equipment such as air conditioners. In addition, its excellent UV resistance (maintaining significant photochromic performance even after 5 h of continuous irradiation) and thermal stability can meet the usage requirements of building materials that are long-term exposed to outdoor environments, extending the service life of the material.